Photo-electrochemical water splitting and hydrogen generation over Ce-CdS/TiO_2/Pt composites coated on FTO substrate

[1*]Ashokrao B. Patil

[1*]Department of Chemistry, K. T. S. P. Mandal's, K. M. C. College, Khopoli–Raigad Maharashtra. PIN- 410203

[*]Corresponding Author, Email: abpatilchem@gmail.com

ORCID ID:- https://orcid.org/0000-0001-9675-8067

[2]Balaso D. Jadhav

[2]Department of Chemistry, Sharadchandra Pawar Mahavidyalaya, Lonand (Shivaji University, Kolhapur), India

Email:jadhavbalaso2472@gmail.com

[3]Akash N. Ghoti

[3]Department of Chemistry, Savitribai Phule Pune University (formerly University of Pune), Ganeshkhind, Pune 411007, India

Email:akashghoti321@gmail.com

[4]Satish K. Pardeshi

[4]Department of Chemistry, Savitribai Phule Pune University (formerly University of Pune), Ganeshkhind, Pune 411007, India

Email: satish.pardeshi@unipune.ac.in

***Abstract*—**Recent studies have shown that the combination of wide-band gap photocatalyst and narrow-band gap semiconductors can collect visible light to enable charge separation and improve the efficiency of H_2 generation. In this article we report excellent solar photocatalytic and photo-electrochemical activity of Ce-CdS/TiO_2/Pt/FTO nano composites towards water splitting and hydrogen generation. Ce-CdS/TiO_2/Pt/FTO nano composites of different Ce content were synthesized with doctorblade followed by Successiveioniclayeradsorptionandreaction(SILAR) Method.Thematerialsthussynthesizedwerecharacterizedusingvariousanalyticaltechniquessuchaspowder X-raydiffractionpattern(PXRD),HRTEM,XPSandRamanspectra.Themorphologyandmicrostructureof Ce-CdSTiO_2/Ptcompositeswereinvestigatedbyscanningelectronmicroscope(SEM).20Ce-CdSTiO_2/Pt/FTOcompositeshowsexcellentactivityforhydrogenevolution(43µmol/h/g).Activitywasfoundtobedependentonthenumberof SILARcyclesandtheimmersiontime.Thedetailedmechanismofsolarwatersplittingon Ce-CdSTiO_2/Pt/FTOwasalsostudied.

Keywords: Sunlight, Hydrogen, Ce-CdS/TiO_2/FTO, Photo-electrochemical, SILAR

.

DOI: 10.48047/ecb/2023.12.si4.1843

1. Introduction

Utilization of clean and renewable energy for human require is one of the demanding areas of research. Sunlight is the excellent source of clean energy and it can be stored for its use upon demand. For this purpose, among the various approaches, solar water splitting over semiconductor materials is the best option for harvesting and store abundant solar energy as clean and easily transportable hydrogen fuel. In this contest several research groups are working in the area of water splitting and hydrogen generation. In particular, TiO_2 has been extensively studied as

one of the typical photocatalyst for water splitting and hydrogen generation [1–5] because of its low cost, nontoxicity, and high chemical stability. In order to enhance activity of TiO_2 towards water splitting and hydrogen generation, it was doped metals. Recently, suppression of carrier recombination and enhancement photocatalytic activity was reported over Sn doped TiO_2 [6]. Similarly, Au/TiO_2 was found to be effective photocatalyst for hydrogen production [7–9]. *Lanterna et.al.* reported enhanced relative rate of hydrogen production over Pd doped TiO_2 among Au, Cu, Pt, Co, Ru and Pd metals [10]. The maximum photocatalytic hydrogen generation of 0.03 mol/h/g over Pt-TiO_2 was observed with a 64W UV light source (λ=254 nm) [11]. Non-metal doping in TiO_2 also increases efficiency of hydrogen generation. Carbon-TiO_2 nanotube was reported as solar photocatalyst to produce hydrogen by means of water splitting. Adding a carbon layer on the surface of TiO_2 nano-tube, improved the quantum efficiency under UV light to 100% and enhanced the absorption capacity under visible-light and extremely suppressed the charge recombination [12]. H_2 production rate of 3.238 $mmolg^{-1}$ h^{-1} were reported over TiO_2 coated carbon fiber as compare to 0.674 $mmolg^{-1}$ h^{-1} by TiO_2 [13]. Hybridization of TiO_2 with activated carbon also enhances photocatalytic production of hydrogen [14]. N-doped TiO_2 also shows photocatalytic properties towards hydrogen production [15]. Possibly, the wide band gap (>3.2eV) of TiO_2 restricts its utilization of the visible light in the solar spectrum, and the high recombination rate of photo-generated electrons and holes in TiO_2 often leads to a low quantum yield and poor photocatalytic activity. Current research has demonstrated that the fusion of a wide-band gap photocatalyst with a narrow-band gap semiconductor can enable charge separation and increase the effectiveness of H_2generation. In this esteem, Trevisan et al [16] developed mesoporous TiO_2 electrodes with in situ deposited PbS/CdS QDs for harvesting light in both the visible and the near-infrared for hydrogen generation. This hetero structure exhibits a photocurrent of 6 $mAcm^{-2}$, leading to 60 $mLcm^{-2}day^{-1}$ hydrogen generation. Similarly, hydrogen production over composite materials such as CdS/TiO_2[17,18], hollow meso-porous CdS@TiO_2@Au microspheres photocatalyst [19], CdS/Pt-TiO_2[20], CuS/TiO_2[21], Au@TiO_2-CdS [22], C_{60} – decorated CdS/TiO_2[23], TiO_2-$Cu(OH)_2$ [24], TiO_2-V_2O_5[25] were also reported. Deposition of composite material on Fluorine doped Tin oxide (FTO) plates is a novel approach to get wireless photo-electrochemical cell and to merge photo-catalysis with electrolysis,which enhances extent of hydrogen production. Shuanglong et al fabricated CdS/TiO_2/FTO nanorod-array film photo-electrodes which has a potential application in solar cells [26]. The enhanced rate of water splitting and hydrogen production was reported over TiO_2-WO_3 nano arrays grown on FTO [27]. Among the small band-gap semiconductors, CdS is an excellent candidate because of its ideal band gap (2.4 eV) and band-edge levels that are capable of driving both the reduction and oxidation of water under visible light irradiation. It has been reported that CdS−TiO_2 composites could show better photo stability and photocatalytic activities than either individual component [17]. The conduction band level of CdS is higher than that of TiO_2, in the visible-light-driven photocatalytic process of proton reduction into H_2, the photo-excited electrons in the CdS conduction band could rapidly transfer to the TiO_2 conduction band through the CdS−TiO_2 interfaces. As such, the effective proton reduction would have to occur on TiO_2 surfaces. Further, loading of metal co-catalysts with CdS allows rapid interfacial electron transfer from the excited semiconductors to the metal co-catalysts, which retards the recombination of photo-generated electron-hole pairs and thereby promotes photocatalytic efficiency. Herein, we present the synthesis of Ce-CdS/ TiO_2/Pt composites of different Ce content coated on FTO plates as wireless photo-electrochemical cell and their enhanced solar photocatalytic activity towards water splitting and hydrogen generation.

2. Experimental methods

2.1 Materials

In present research work, Titanium (IV) oxide nano particles (21nm) (assay 99.5%, Aldrich), Fluorine doped tin oxide coated glass slide (735167-1EA, Aldrich) Cadmium nitrate tetrahydrare (> 99.5%, Alfa Aesar), Sodium sulphide (>99.5%, Merck), Cerium (IV) nitrate (assay 98.5%, Merck) and other required chemicals are of analytical grade, obtained from Merck Limited, Mumbai, India and were used without further purification.

2.2. Fabrication of Ce-CdS-TiO_2/Pt/FTO composite

The TiO_2/Pt/FTO was initially obtained by coating TiO_2 paste on a2.0cm surface of FTO (2.5 cm × 1.0 cm dimension) substrate by doctor blade technique and then drying at 80°C followed by applying Pt paste on a0.5cm surface of FTO substrate at one end and then calcination at 450^{o}C for 10min. The TiO_2/Pt/FTO was then sensitized with CdS by successive ionic layer adsorption and reaction (SILAR) method. In a typical process, 0.1M aqueous solution of cadmium nitrate tetra-hydrare and 0.1M Na_2S in methanol/water (50/50 V/V) solution was firstly prepared. Then the as prepared TiO_2/Pt/FTO cell was dispersed in Cadmium nitrate solution for 1 min until the Cd^{2+}ions were adsorbed on the TiO_2 film. Then the loose part of adsorbed Cd^{2+}ions was removed by rinsing with Millipore water. Further, the TiO_2/Pt/FTO adsorbed with Cd^{2+}were immersed in Na_2S solution for 1 min, thus the S^{2-}ions were adsorbed and reacted with Cd^{2+}ions to form CdS during the immersion process. By rinsing with Millipore water, the superfluous S^{2-}ions were removed, leaving the CdS on TiO_2 surface. Then, the CdS-TiO_2/Pt/FTO film was dried at 60^{o}C in oven for 10 min. This is the single SILAR deposition cycle. In order to optimize the thickness of CdS-TiO_2 film, SILAR procedure was repeated 1 to 7 times. After CdS deposition the sample was coated with ZnS by dipping alternately into 0.1 M $Zn(CH_3COO)_2$ (in water) and 0.1M Na_2S solutions for 1 min/dip, rinsing with Millipore water between dips (two cycles), followed by drying at 60^{o}C in oven for 10 min.The Ce-CdS/TiO_2/FTO composites of different Ce contents were obtained by dipping previously fabricated CdS-TiO_2 films in Cerium (IV) nitrate precursor solution having appropriate concentrations (1000 to 6000ppm) in methanol/water (50/50 V/V), as per **Table 1**.

Table 1: Syntheses Ce-CdS/TiO_2/FTO composites of different Ce content

Concentration of Cerium (IV) nitrate (ppm)	Photocatalyst
0	CdS/TiO_2/Pt/FTO
1000	10Ce-CdS/TiO_2/Pt/FTO
2000	20Ce-CdS/TiO_2/Pt/FTO
3000	30Ce-CdS/TiO_2/Pt/FTO
4000	40Ce-CdS/TiO_2/Pt/FTO
5000	50Ce-CdS/TiO_2/Pt/FTO
6000	60Ce-CdS/TiO_2/Pt/FTO

The as-synthesized Ce-CdS/TiO_2/Pt/FTOhetro structure materials were characterized by using different analytical techniques. Powder X-ray diffraction (PXRD) patterns were collected from a PAN analytical X'pert Pro dual goniometer X-ray diffractometer, using Cu-Kα (1.5418 Å) radiation with a Ni filter, and the data were collected using a flat holder in Bragg–Brentano geometry (0.2°). HRTEM of the materials was conducted on a FEITECNAI 3010 electron microscope operating at 300 kV (Cs =0.6 mm; 1.6 Å resolution). Raman spectra of the samples were analyzed with a Horiba JY LabRAM HR 800 Raman spectrometer coupled with a microscope in reflectance mode with a 633 nm excitation laser source and a spectral resolution of 0.3 cm^{-1}. XPS measurements were taken with a Custom-built ambient pressure XPS system20 (Prevac, Poland) and equipped with a VG Scienta SAX 100 emission controller monochromator using an Al Kα anode (1486.6 eV) in transmission lens mode. The morphology and microstructure of the photocatalysts were examined by scanning electron microscope (SEM)

2.3 Water splitting and Hydrogen generation study

As synthesized Ce-CdS/TiO_2/Pt/FTO composites were used for water splitting and hydrogen generation under one sun conditions using solar simulator. The mixture of 0.25 M Na_2S and 0.35 M Na_2SO_3 aqueous solution as the sacrificial hole scavenger was used as the electrolyte to prevent photocorrosion of photocatalyst. An Oriel

Instruments solar simulator equipped with a 300 W xenon arc lamp system with an AM 1.5 cut-off filter as the irradiation source was employed. The above filter can be easily replaced with any other wavelength cut-off filter to alter the radiation wavelength regime. The reaction vessel was kept 20 cm away from the light source to ensure the one sun condition, as suggested by the Oriel solar simulator manual. This was further confirmed by the current, as measured by a lux meter. Cool air circulation was employed to maintain a constant temperature (27 °C) during irradiation. Gas analysis was carried out by regular sampling every hour, and a gas chromatograph (GC) equipped with a TCD detector (Agilent 7890) was employed for quantitative analysis

3. Result and discussion

3.1. Activity of Ce-CdS/TiO_2/Pt/FTO composites towards solar water splitting

Solar photocatalytic activity of Ce-CdS/TiO_2/Pt/FTO was evaluated by means of photocatalytic water splitting and hydrogen generation and results are summarized in **Fig.1**.

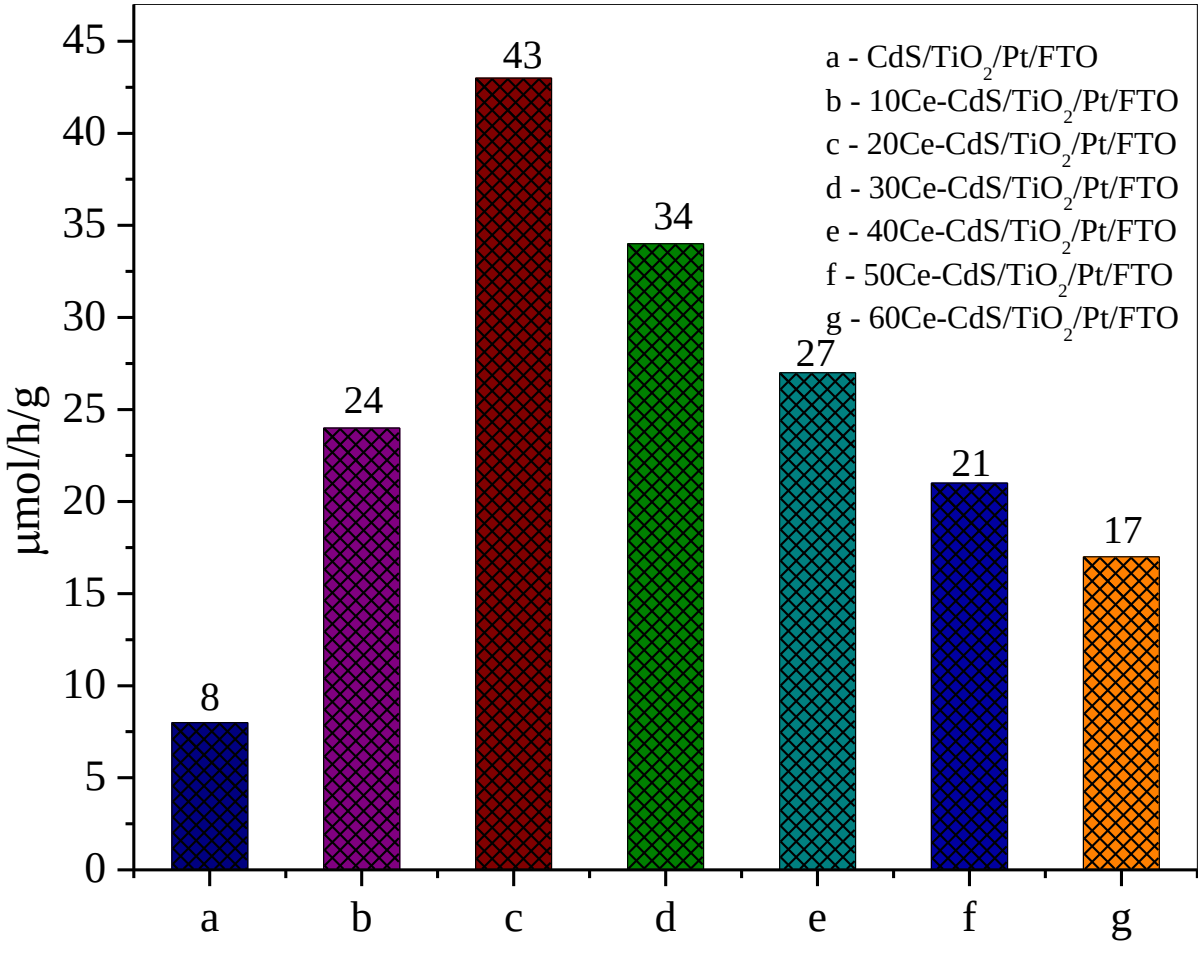

Fig.1: Solar photocatalytic hydrogen production over Ce-CdS/TiO_2/Pt/FTO composites

CdS/TiO_2/Pt/FTO found to generate 8 µmol/h/g of hydrogen in solar light. When CdS/TiO_2/Pt/FTO is doped with Cerium, the extent of solar hydrogen generation drastically increases with increase in Ce content up to 20mg of Ce (20CdS/TiO_2/FTO), which produces 43 µmol/h/g of hydrogen in solar light (**Fig.1**). Further increase in Ce content shows negative effect and activity was found to decrease. This may be attributed to fact that, doping of Ce in CdS-TiO_2 produces Schottky barrier at the interface between CdS and TiO_2 resulting in an efficient channeling of

electrons from the bulk of CdS to the newly formed interface which is responsible to suppress electron–hole pair recombination. The photocatalytic activity of Ce-CdS-TiO_2/Pt/FTO composites was found to depend on number of SILAR cycles. With increase in SILAR cycles, the thickness of Ce-CdS-TiO_2 film increases and PCD efficiency is also increase and as the thickness of Ce-CdS-TiO_2 composites film on FTO substrate exceeds the optimum size (10 to 12μ), activity found to decrease (**Table 2**).This is due to fact that, as the thickness of semiconductor composite increases due to deposition of Ce-CdS layer on the TiO_2, the synergetic effect gets discontinued as a result of this, there is isolation of TiO_2 phase.

Number of SILAR cycles	*Thickness of Ce-CdS /TiO_2 composites (μ)*	H_2 Production *(μ/mol/h/g)*
1	2.8	12
2	4.7	15
3	6.5	19
4	8.2	25
5	9.8	39
6	10.2	43
7	12.5	41

Table 2: Dependence of photocatalytic activity on number of SILAR cycles and hence thickness of Ce-CdS /TiO_2 composites on FTO substrate

3.1.1 Mechanism of Solar water splitting

When the Ce-CdS/TiO_2/Pt/FTO composite was illuminated with solar radiation, Ce-CdS/TiO_2 function as photocatalyst. CdS absorbing light in the near visible region allows the promotion of some electrons to its CB, leading to the formation of electron-hole pairs. Then the electrons promoted in the CB of the CdS are injected in the CB of TiO_2, while the VB holes are staying in CdS. At the same time TiO_2 is absorbing the UV light producing new electron holes pairs. The injection of the latter electrons in the CB of the coupled semiconductor facilitates the electron-holes separation preventing charge recombination.The CdS alone is unstable towards the photo-corrosion as a result of the S^{2-} oxidation by the photo-generated holes and the consequent release of Cd^{2+} into the solution. However, this is hindered by performing the reaction in presence of a hole scavenger (S^{2-} and SO_3^{2-}) in the electrolyte. Doping of Ce^{4+} in CdS further assist the visible light absorption and hence increases the activity of composite towards hydrogen generation. Owing to the narrow band-gap of CdS and the synergistic effect of ternary phase, the Ce-CdS/TiO_2 can absorb more visible light, which provides a more extensive range of adsorption spectrum than bare TiO_2 and CdS /TiO_2 composites. Further, Ce dopant of Ce-CdS-TiO_2 surface behaves like electron sinks, which provide sites for the accumulation of electrons, and then improve the separation of photo-generated electrons and holes, which is favorable for its solar photocatalytic activity towards hydrogen production. Further it is to be noted that, Ce-CdS-TiO_2/Pt/FTO act as a photo-electrochemical cell, where Ce-CdS-TiO_2 act as photo-anode whereas Pt acts as cathode and FTO plays the role of electron carrier from anode to cathode (**Scheme**

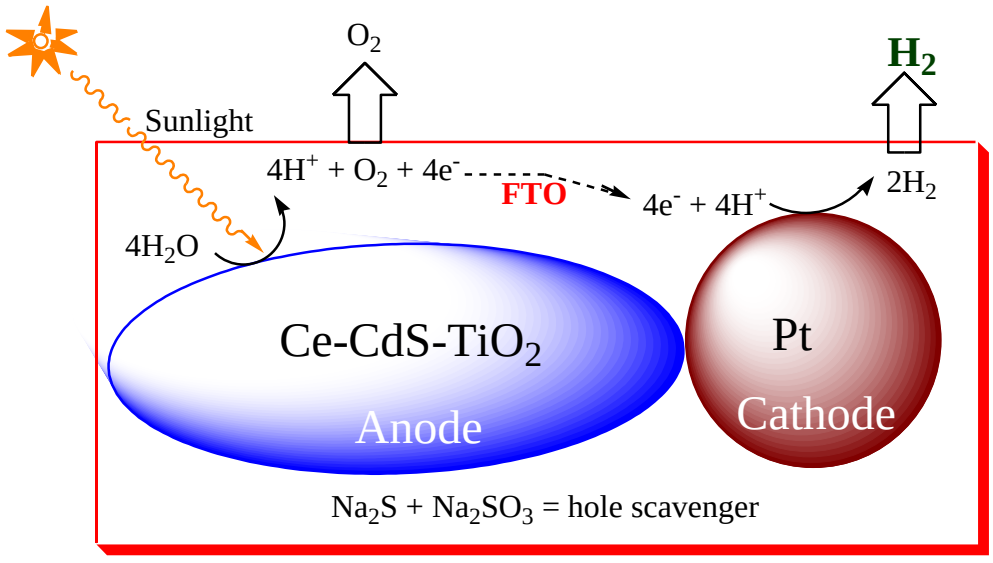

1).

Scheme 1: Mechanism of photo-electrochemical water splitting over Ce-CdSTiO_2/Pt/FTO

As soon as water containing Ce-CdS-TiO_2/Pt/FTO composites and electron scavenger is exposed to visible light, at anode oxidation of water takes place to evolve oxygen and electrons. FTO carries electrons from anode to cathode. At cathode (Pt) reduction of H^+ takes place to generate Hydrogen (**Scheme 1**).

3.2. Characterization of Ce-CdS /TiO_2 photocatalyst cum photoanode coated on FTO substrate

As 20Ce-CdS/TiO_2/Pt/FTO photo-electrochemical cell was found to be more active towards water splitting and hydrogen generation, more emphasis was given for its characterization by means of various techniques.

3.2.1. XRD analysis

In order to identify the crystal structure of TiO_2, CdS-TiO_2, and Ce-CdS-TiO_2 composites coated on FTO substrate, XRD analysis is done and results are depicted in **Fig. 2a-d.**

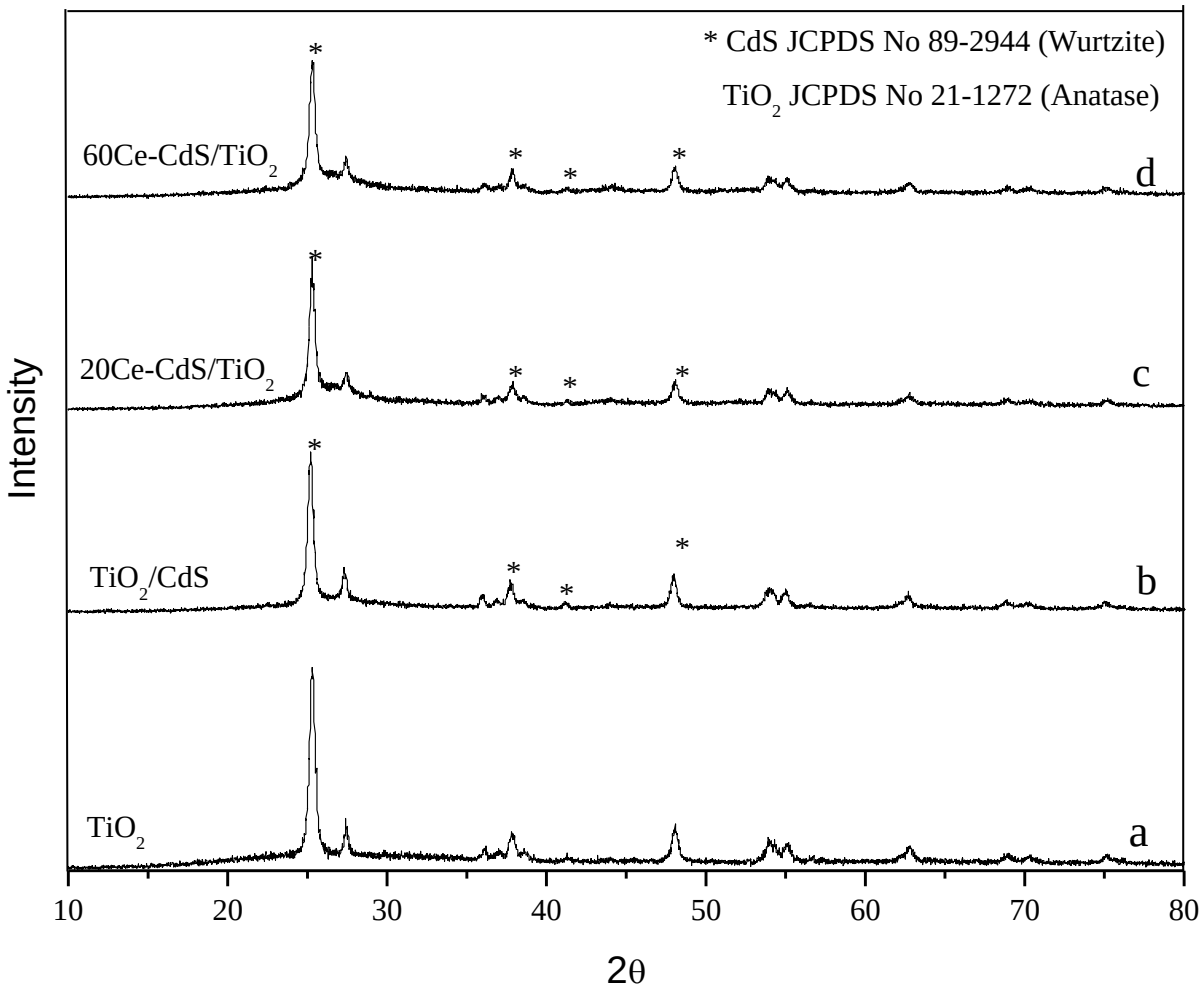

Fig.2: XRD pattern of (a) TiO_2 (b) TiO_2/CdS, (c) 20Ce-CdS/TiO_2, (d) 60Ce-CdS/TiO_2

TiO_2 shows the characteristic diffraction peaks of anatase TiO_2 (JCPDS card no. 21-1272) **(Fig.2a).** Upon deposition with CdS nanoparticles, the XRD patterns exhibit the characteristic peaks of hexagonal CdS (JCPDS card no. 89-2944) **(Fig.2b)**. It is to be noted that, all peaks from the TiO_2 sample before CdS deposition remained present in CdS-TiO_2, and some of the CdS peaks overlap with the TiO_2 peaks. As the extent of Ce is very less, no extra peaks for CeS_2 were observed however, XRD patterns of CdS-TiO_2 **(Fig.2b),**20Ce-CdS-TiO_2 **(Fig.2c),** and 60Ce-CdS-TiO_2 **(Fig.2d)** found to be progressively broader and smalleras compare to that of TiO_2.

3.2.2 SEM Analysis of 20Ce-CdS/TiO_2/Pt/FTO film

The thickness and morphology of 20Ce-CdS-TiO_2/Pt/FTO films was investigated with SEM analysis (**Fig.3**).

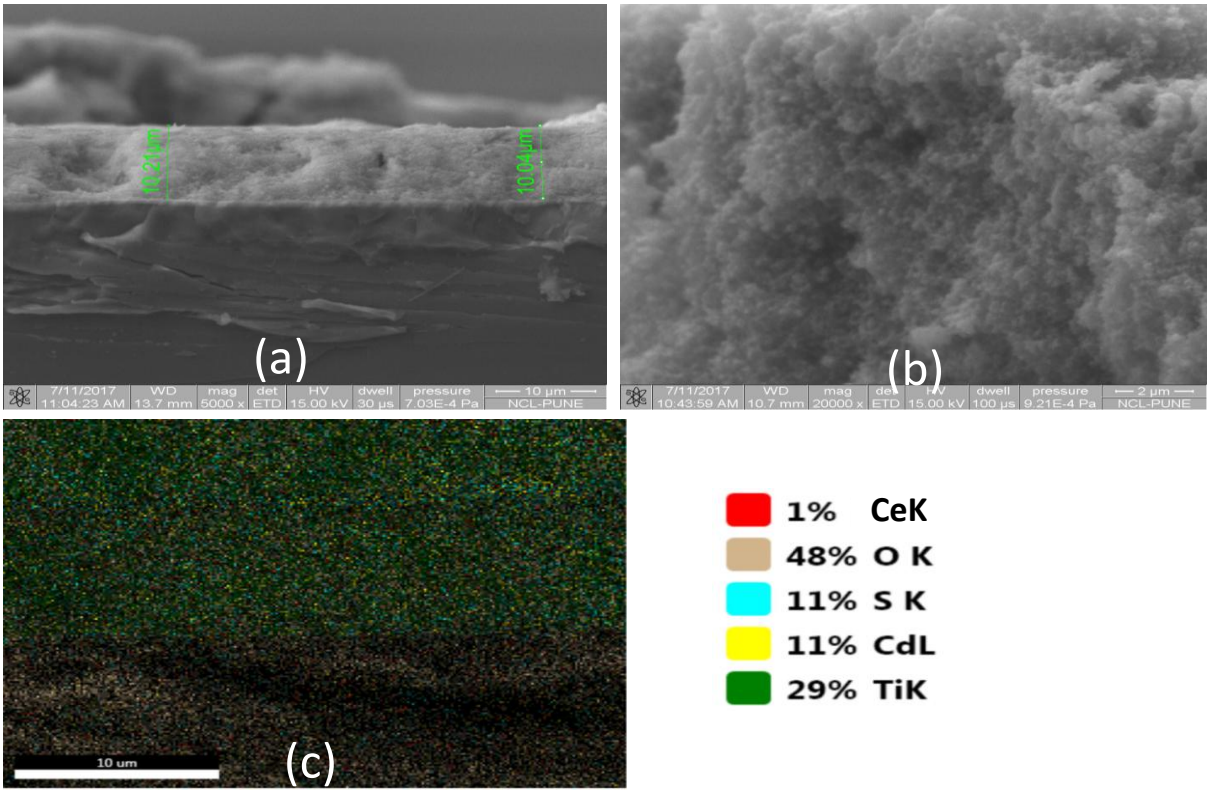

Fig.3: SEM images and elemental mapping of 20Ce-CdS/TiO_2/FTO composite: (a) side view (b) Top view (c) Elemental mapping

It can be seen that the FTO substrate is covered uniformly with Ce-CdS/TiO_2 film with the thickness of 10.2µm (**Fig.3a**).The surface of Ce-CdS/TiO_2 film was found to be porous and spongy nature (**Fig.3b**). The porous-like structure having fluffy morphology favours the adsorption of substrate molecules involved in the photocatalytic process and also increases the surface area of photocatalyst. Elemental mapping of Ce-CdS-TiO_2/FTO suggest the presence of Ce along with Ti, Cd, S and O **(Fig.3c).**

3.2.3 HR-TEM analysis of 20Ce-CdS/TiO_2

The morphology of 20Ce-CdS/TiO_2 was further investigated by HR-TEM. The HR-TEM images of different magnifications are shown in **Fig.4.** The HR-TEM images reveal that the CdS nanoparticles are intimately contacted with the TiO_2 nanoparticle shells with clear CdS−TiO_2 interfaces.
The observed lattice spacing of 0.35 nm corresponding to the (001) facet of anatase TiO_2, a lattice spacing of 0.318 nm corresponding to the (101) facet of hexagonal CdS, and another lattice spacing of 0.33 nm corresponding to the (111) facet of crystalline CeS_2. It also suggests that the particle size of CdS and CeS_2 deposited by SILAR method lies in the range of 20 to 50nm.

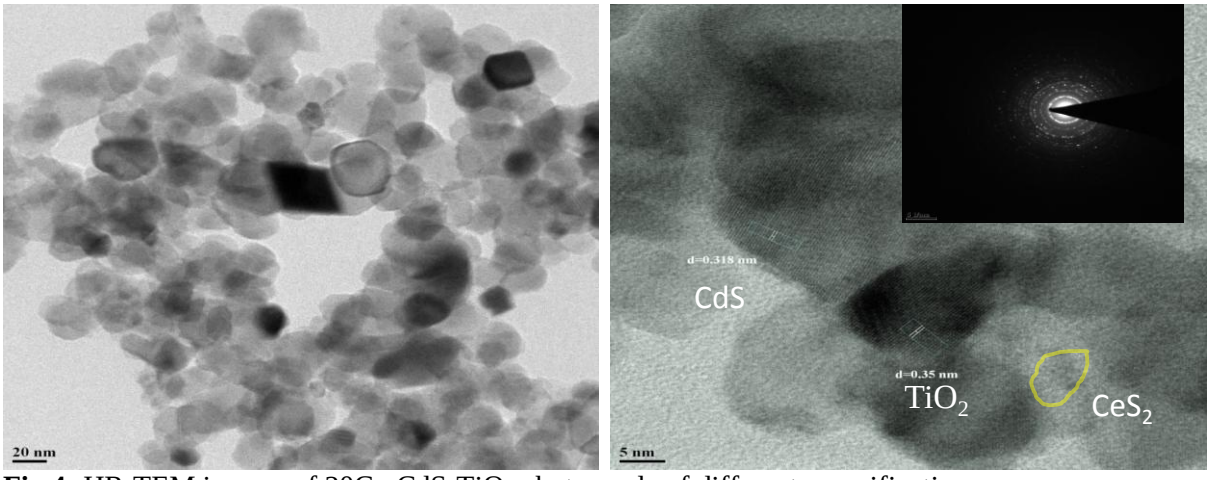

Fig.4: HR-TEM images of 20Ce-CdS-TiO_2 photoanode of different magnifications

3.2.4 XPS analysis of 20Ce-CdS/TiO_2photoanode

The composition of 20Ce-CdS/$TiO_2$was investigated by X-ray photoelectron spectra (XPS) and results are displayed in **Fig.5a-f**. Full scan XPS of 20Ce-CdS/TiO_2 is shown in **Fig.5a.**The high resolution XPS of O1s region of 20Ce-CdS/TiO_2**(Fig.5b)** show prominent peaks centred at 529.85eV for O^{2-} ions of TiO_2 and 531.54eV for lower valence oxygen or adsorbed oxygenor adsorbed oxygen. The high resolution XPS of S2p region of 20Ce-CdS/TiO_2showsthe peaks positioned at 161.4eV and 162.4eV are assigned to the S $2p_{3/2}$ and S $2p_{1/2}$ electronic states of sulphur respectively**(Fig.5c)**. The XPS peak at 169.6eV is attributed to SO_4^{--} species formed on the surface of film due air oxidation.

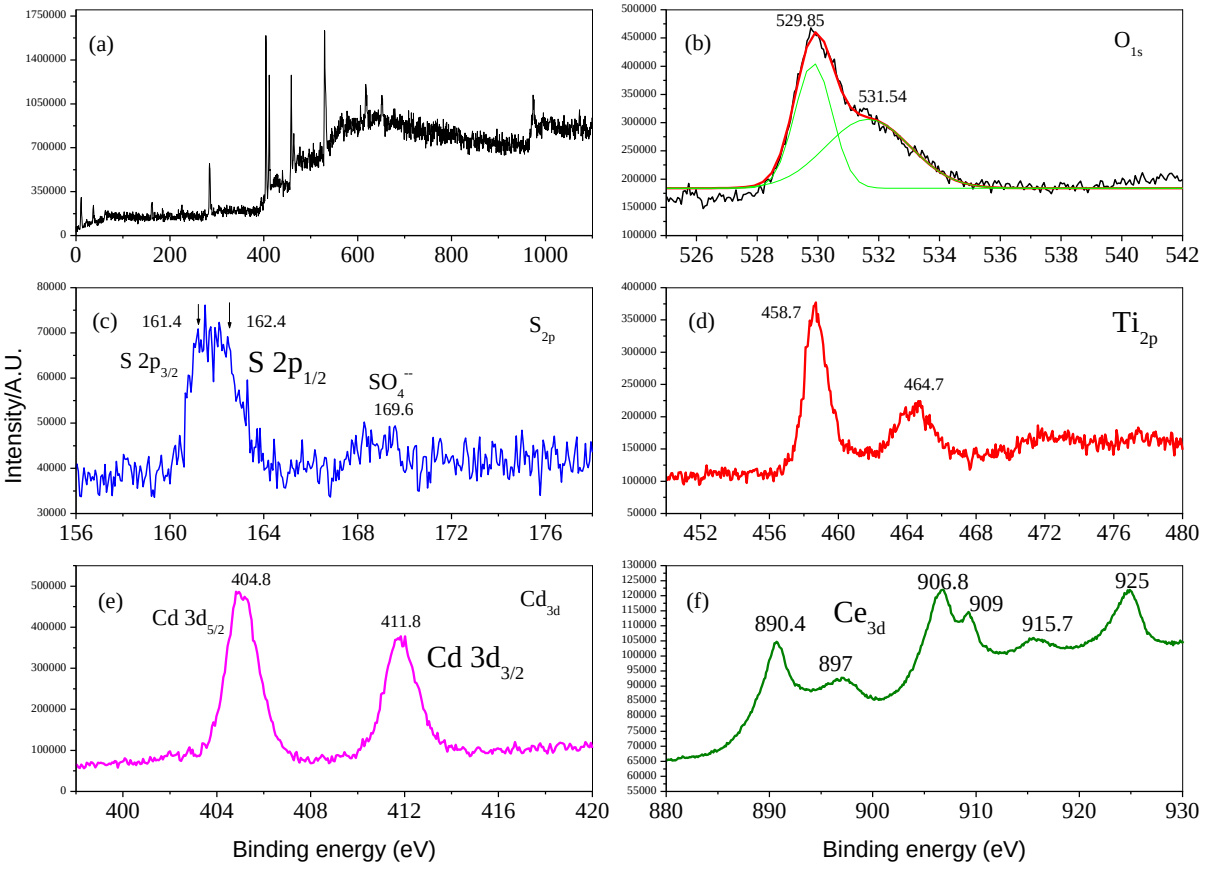

Fig.5: XPS of 20Ce-CdS-TiO_2: (a) Full scan XPS of 20Ce-CdS-TiO_2, high resolution XPS of (b) O1s region, (c) S2p region, (d) Ti2p region, (e) Cd3d region, (e) Ce3d region.

Fig.5d shows the Ti2p core level BE, which appears at 458.7 ± 0.1 eV. **Fig. 5e** demonstrates the high-resolution XPS scan of Cd3d region of the 20Ce-CdS/TiO_2**.** The facet peaks at 404.8eV (Cd $3d_{5/2}$) and 411.8 eV (Cd $3d_{3/2}$) can be endorsed to Cd^{2+} species in 20Ce-CdS/TiO_2. High resolution XPS scan of Ce_{3d} region shows prominent peaks centred at 890.4 and 897eV are assigned to $3d_{5/2}$ state of Ce^{4+} ion and peaks centred at 906.8, 909, 915.7 and 925eV are assigned to $3d_{3/2}$ state of Ce^{4+} ion in 20Ce-CdS/TiO_2 **(Fig. 5f).**

3.2.5 Raman spectra

Raman spectroscopy is a powerful tool to analyze the crystalline quality and the integration aspects of the composite material. **Fig. 6** shows the comparative Raman spectra of the bare TiO_2, CdS-TiO_2, 20Ce-CdS/TiO_2 and 60Ce-CdS/TiO_2 composites.

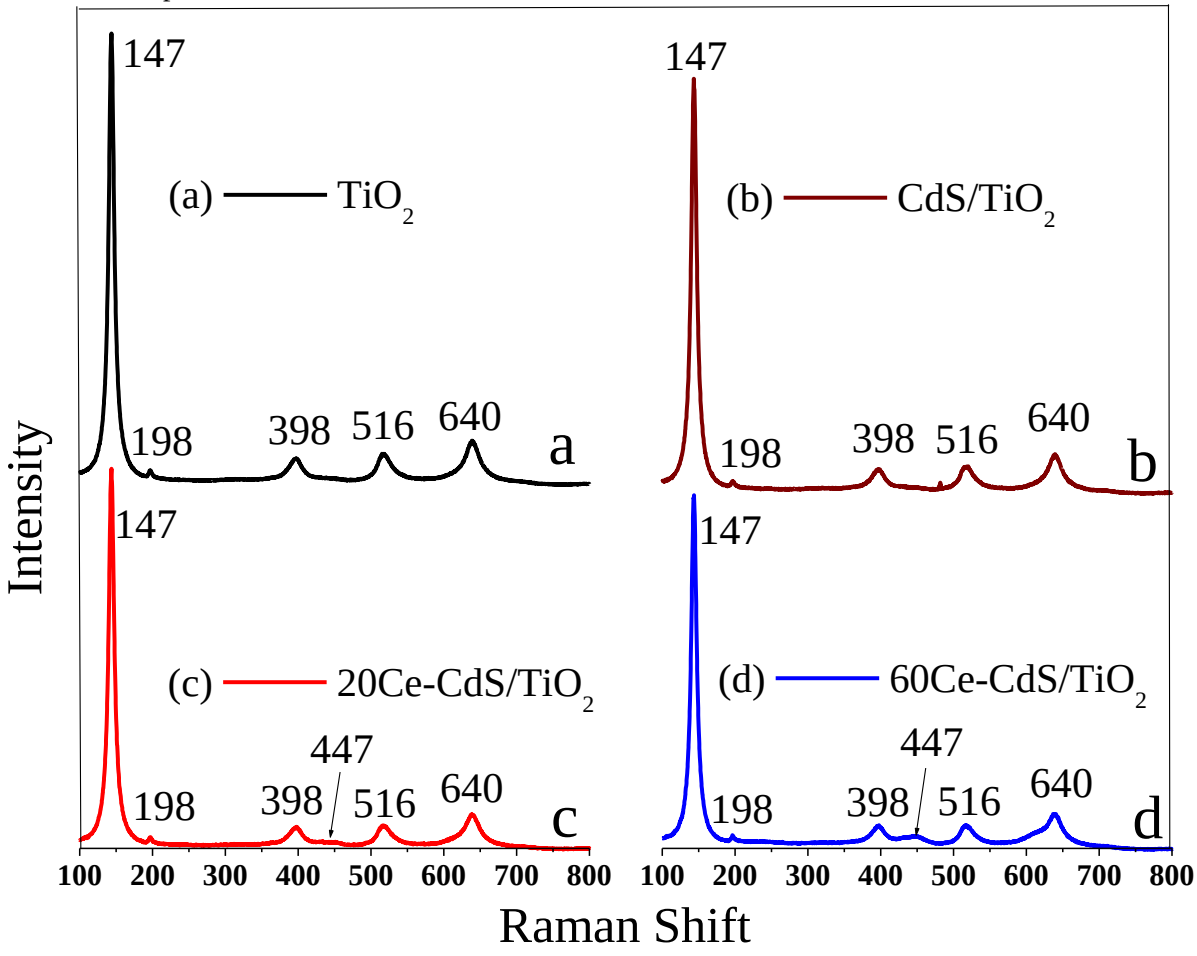

Fig.6: Raman spectra of (a) TiO_2 (b) TiO_2/CdS, (c) 20Ce-CdS/TiO_2, (d) 60Ce-CdS/TiO_2composite.
All the samples shows the fundamental modes of TiO_2, observed around 147 (Eg), 198 (Eg), 398 (B1g), 516 (A1g + B1g), and 640 (Eg) cm^{-1} for the anatase phase (**Fig. 6a-d**). When TiO_2 is deposited with CdS the Raman peaks of TiO_2 becomes broader and smaller **(Fig.6b-d)**.Raman spectrum of 20Ce-CdS/TiO_2 and60Ce-CdS/TiO_2 composites becomes broader and smalleralsoshows new Raman feature at 447.5 cm^{-1} **(Fig.6c, d)**.

4. Conclusions

Ce-CdS/TiO_2/Pt/FTO composites of different Cerium content were synthesized by doctor blade followed by SILAR

method. 20Ce-CdS/TiO_2/Pt/FTO composite shows excellent photocatalytic activity towards hydrogen generation by means of water splitting in solar light. SEM analysis supports the uniform thickness of composite film of 10μm to 12μm in case of 20Ce-CdS/TiO_2/Pt/FTO photocatalyst, attributed to its better photocatalytic activity. XPS, XRD, Raman Spectra, SEM etc. are important techniques to tune the composition and morphology of photocatalyst and to enhance their photocatalytic activity. Production of green hydrogen to the bulk level using solar photocatalytic water splitting technique needs further research and development.

Acknowledgements

Ashokrao B. Patil is grateful to Indian Academy of Sciences Bengaluru, Indian National Science Academy, New Delhi and The National Academy of Sciences, Allahabad (IASc-INSA-NASI) for awarding SRF. Authors are also thankful to National Chemical Laboratories, Pune, (India) for providing the necessary facilities.

REFERENCES

1. H. Kim, B.L. Yang, Effect of seed layers on TiO_2 nanorod growth on FTO for solar hydrogen generation, Int. J. Hydrogen Energy. 40 (2015) 5807–5814. https://doi.org/10.1016/j.ijhydene.2015.03.007.
2. G. Li, J. Huang, C. Xue, J. Chen, Z. Deng, Q. Huang, Z. Liu, C. Gong, W. Guo, R. Cao, Facile Synthesis of Oriented Feather-like TiO_2 Bundle Catalysts for Efficient Photocatalytic Water Splitting, Cryst. Growth Des. 19 (2019) 3584–3591. https://doi.org/10.1021/acs.cgd.9b00495.
3. P. Afanasiev, Transfer of stored electrons between TiO_2 polymorphs during photocatalytic H2 production in methanol–water medium, Appl. Catal. A Gen. 598 (2020) 117548. https://doi.org/10.1016/j.apcata.2020.117548.
4. J. Zhang, Y. Lei, S. Cao, W. Hu, L. Piao, X. Chen, Photocatalytic hydrogen production from seawater under full solar spectrum without sacrificial reagents using TiO_2 nanoparticles, Nano Res. 15 (2022) 2013–2022. https://doi.org/10.1007/s12274-021-3982-y.
5. M. Salazar-Villanueva, L.R. Morales-Juárez, O. Flores Sánchez, A. Cruz-López, A. Tovar-Corona, O. Vázquez-Cuchillo, Enhanced photocatalytic water splitting hydrogen production on TiO2 nanospheres: A theoretical- experimental approach, J. Photochem. Photobiol. A Chem. 434 (2023). https://doi.org/10.1016/j.jphotochem.2022.114212.
6. H. Wang, L. Song, L. Yu, X. Xia, Y. Bao, M. Lourenco, K. Homewood, Y. Gao, Charge transfer between Ti^{4+}, Sn^{4+} and Pt in the tin doped TiO_2 photocatalyst for elevating the hydrogen production efficiency, Appl. Surf. Sci. 581 (2022) 152202. https://doi.org/10.1016/j.apsusc.2021.152202.
7. G. Pahlevanpour, H. Bashiri, Kinetic Monte Carlo simulation of hydrogen production from photocatalytic water splitting in the presence of methanol by 1 wt% Au/TiO_2, Int. J. Hydrogen Energy. 47 (2022) 12975–12987. https://doi.org/10.1016/j.ijhydene.2022.02.061.
8. N. Kunthakudee, T. Puangpetch, P. Ramakul, K. Serivalsatit, M. Hunsom, Light-assisted synthesis of Au/TiO_2 nanoparticles for H_2 production by photocatalytic water splitting, Int. J. Hydrogen Energy. 47 (2022) 23570–23582. https://doi.org/10.1016/j.ijhydene.2022.05.150.
9. J. Fang, S.W. Cao, Z. Wang, M.M. Shahjamali, S.C.J. Loo, J. Barber, C. Xue, Mesoporous plasmonic Au-TiO 2 nanocomposites for efficient visible-light-driven photocatalytic water reduction, Int. J. Hydrogen Energy. 37 (2012) 17853–17861. https://doi.org/10.1016/j.ijhydene.2012.09.023.
10. A.S. Hainer, J.S. Hodgins, V. Sandre, M. Vallieres, A.E. Lanterna, J.C. Scaiano, Photocatalytic Hydrogen Generation Using Metal-Decorated TiO_2: Sacrificial Donors vs True Water Splitting, ACS Energy Lett. 3 (2018) 542–545. https://doi.org/10.1021/acsenergylett.8b00152.
11. R.P. Antony, T. Mathews, C. Ramesh, N. Murugesan, A. Dasgupta, S. Dhara, S. Dash, A.K. Tyagi, Efficient photocatalytic hydrogen generation by Pt modified TiO_2 nanotubes fabricated by rapid breakdown anodization, Int. J. Hydrogen Energy. 37 (2012) 8268–8276. https://doi.org/10.1016/j.ijhydene.2012.02.089.
12. F. Almomani, M. Shawaqfah, M. Alkasrawi, Solar-driven hydrogen production from a water-splitting cycle based on carbon-TiO_2 nano-tubes, Int. J. Hydrogen Energy. 47 (2022) 3294–3305. https://doi.org/10.1016/j.ijhydene.2020.12.191.
13. T.L. Nguyen, T.H. Pham, Y. Myung, S.H. Jung, M.H. Tran, M.G. Mapari, Q. Van Le, M.V. Nguyen, T.T.H. Chu, T. Kim, Enhanced photocatalytic activity in water splitting for hydrogen generation by using TiO_2

coated carbon fiber with high reusability, Int. J. Hydrogen Energy. 47 (2022) 41621–41630. https://doi.org/10.1016/j.ijhydene.2022.06.025.

14. S. Sekar, V. Preethi, V.S. Srivishnu, S. Saravanan, S. Lee, Highly-efficient photocatalytic activity of TiO_2-AC nanocomposites for hydrogen production from sulphide wastewater, Int. J. Hydrogen Energy. 47 (2022) 40275–40285. https://doi.org/10.1016/j.ijhydene.2022.02.019.
15. Y.V. Divyasri, N. Lakshmana Reddy, K. Lee, M. Sakar, V. Navakoteswara Rao, V. Venkatramu, M.V. Shankar, N.C. Gangi Reddy, Optimization of N doping in TiO2 nanotubes for the enhanced solar light mediated photocatalytic H_2 production and dye degradation, Environ. Pollut. 269 (2021) 116170. https://doi.org/10.1016/j.envpol.2020.116170.
16. R. Trevisan, P. Rodenas, V. Gonzalez-Pedro, C. Sima, R.S. Sanchez, E.M. Barea, I. Mora-Sero, F. Fabregat-Santiago, S. Gimenez, Harnessing infrared photons for photoelectrochemical hydrogen generation. A PbS quantum dot based "quasi-artificial leaf," J. Phys. Chem. Lett. 4 (2013) 141–146. https://doi.org/10.1021/jz301890m.
17. G.S. Li, D.Q. Zhang, J.C. Yu, A new visible-light photocatalyst: CdS quantum dots embedded mesoporous TiO_2, Environ. Sci. Technol. 43 (2009) 7079–7085. https://doi.org/10.1021/es9011993.
18. F. Tian, D. Hou, F. Hu, K. Xie, X. Qiao, D. Li, Pouous TiO_2 nanofibers decorated CdS nanoparticles by SILAR method for enhanced visible-light-driven photocatalytic activity, Appl. Surf. Sci. 391 (2017) 295–302. https://doi.org/10.1016/j.apsusc.2016.07.010.
19. W. Yuan, Z. Zhang, X. Cui, H. Liu, C. Tai, Y. Song, Fabrication of Hollow Mesoporous CdS@TiO_2@Au Microspheres with High Photocatalytic Activity for Hydrogen Evolution from Water under Visible Light, ACS Sustain. Chem. Eng. 6 (2018) 13766–13777. https://doi.org/10.1021/acssuschemeng.8b01787.
20. H. Park, Y.K. Kim, W. Choi, Reversing CdS preparation order and its effects on photocatalytic hydrogen production of CdS/Pt-TiO_2 hybrids under visible light, J. Phys. Chem. C. 115 (2011) 6141–6148. https://doi.org/10.1021/jp2015319.
21. M. Chandra, K. Bhunia, D. Pradhan, Controlled Synthesis of CuS/TiO_2 Heterostructured Nanocomposites for Enhanced Photocatalytic Hydrogen Generation through Water Splitting, Inorg. Chem. 57 (2018) 4524–4533. https://doi.org/10.1021/acs.inorgchem.8b00283.
22. J. Fang, L. Xu, Z. Zhang, Y. Yuan, S. Cao, Z. Wang, L. Yin, Y. Liao, Au @ TiO_2 − CdS Ternary Nanostructures for E ffi cient Visible-Light- Driven Hydrogen Generation, (2013).
23. Z. Lian, P. Xu, W. Wang, D. Zhang, S. Xiao, X. Li, G. Li, C60-decorated CdS/TiO_2 mesoporous architectures with enhanced photostability and photocatalytic activity for H_2 evolution, ACS Appl. Mater. Interfaces. 7 (2015) 4533–4540. https://doi.org/10.1021/am5088665.
24. H. She, X. Ma, K. Chen, H. Liu, J. Huang, L. Wang, Q. Wang, Photocatalytic H2 production activity of TiO_2 modified by inexpensive $Cu(OH)_2$ cocatalyst, J. Alloys Compd. 821 (2020). https://doi.org/10.1016/j.jallcom.2019.153239.
25. L. Gnanasekaran, S. Rajendran, H. Karimi-Maleh, A.K. Priya, J. Qin, M. Soto-Moscoso, S. Ansar, C. Bathula, Surface modification of TiO_2 by adding V_2O_5 nanocatalytic system for hydrogen generation, Chem. Eng. Res. Des. 182 (2022) 114–119. https://doi.org/10.1016/j.cherd.2022.03.046.
26. S. Feng, J. Yang, M. Liu, H. Zhu, J. Zhang, G. Li, J. Peng, Q. Liu, CdS quantum dots sensitized TiO_2 nanorod-array-film photoelectrode on FTO substrate by electrochemical atomic layer epitaxy method, Electrochim. Acta. 83 (2012) 321–326. https://doi.org/10.1016/j.electacta.2012.07.130.
27. H. Ali, N. Ismail, A. Hegazy, M. Mekewi, A novel photoelectrode from TiO_2-WO_3 nanoarrays grown on FTO for solar water splitting, Electrochim. Acta. 150 (2014) 314–319. https://doi.org/10.1016/j.electacta.2014.10.142.